Quantitative Light Element Analysis Using an Energy-dispersive Detector

2*—Continuum Removal and Peak Deconvolution

D. J. Bloomfield and G. Love
School of Materials Science, University of Bath, Bath BA2 7AY, UK

Techniques for analysing light elements by energy-dispersive spectrometry are discussed and a new approach is proposed. Firstly, a method for predicting the x-ray continuum level is developed. It is based on the use of a reference standard and, unlike other methods, is accurate below 1.5 keV. When combined with methods for dealing with spectrum artefacts, this approach allows the calculation of background levels down to 0.1 keV. Attention is then given to the problem of overlap, which is particularly important in light element analysis. Various methods for deconvolution of peaks are considered and a technique is adopted based on least-squares fitting of standard peak profiles. The effects of count statistics and computational accuracy on the final results are discussed. Some practical overlap situations are examined to discover the level of accuracy which can be expected.

INTRODUCTION

Quantitative electron-probe microanalysis requires reliable x-ray intensity measurements to be made on specimens and standards. In energy-dispersive (ED) analysis this involves processing the recorded spectrum, firstly to separate the characteristic x-ray peaks from background, and secondly to deal with any overlap from neighbouring x-ray lines. Various processing methods exist[1,2] but whilst most appear to work satisfactorily for elements of atomic number (Z) above 11, they remain unproven for light elements ($5 < Z < 11$). Indeed, evidence[3] suggests that many may be completely inappropriate. It has been shown that this may be partly due to factors unique to soft x-ray analysis, such as background artefacts and inaccurate dead-time corrections. These have been dealt with in a previous paper[4] and here we focus attention on further problems associated with continuum removal and peak deconvolution.

There are essentially two ways of dealing with the spectrum background, the first involving mathematical filtering and the second based on predicting background shape. One approach to mathematical filtering, described by Statham[5] and McCarthy and Schamber,[6] employs a 'top hat' convolution to produce an approximate separation of the highly curved peaks from the relatively flat background. The resulting spectrum is greatly distorted, but by applying the same convolution to the spectrum from the standard a reliable peak-intensity ratio may be obtained using least-squares fitting. This technique deals automatically with deconvolution of overlapping peaks. The second method[7] involves setting up a model to describe the shape of the background which takes into account the generated continuum intensity, absorption of continuum in the spectrum, spectrometer efficiency, noise contribution and any spectrum artefacts. The deconvolution of overlapping peaks can then be dealt with separately by using least-squares fitting of library spectra or of generated Gaussian peaks; alternatively, overlap factors may be employed.

It is not obvious which is the best approach to adopt for processing soft x-ray spectra, but for the following reasons we have chosen to use the second method: background modelling followed by deconvolution using least-squares analysis. Firstly, digital filtering does not give an explicit background level and any assessment of detection sensitivity requires accurate measurement of both peak and background intensity. Secondly, it is impractical to obtain reliable estimates of statistical errors when both filtering and fitting are employed.[5] Thirdly, filtering would be difficult in the vicinity of the carbon peak where the low-energy cut-off introduces a discontinuity in the spectrum. Finally, it was felt that background modelling was the more flexible approach, offering greater scope for development.

The investigation was performed using an EDAX 711 analyser with an ECON detector attached to a JEOL JXA 50A electron-probe microanalyser. Measurement of light elements has been undertaken using a thin Formvar detector window rather than by operating in the windowless mode.

PREDICTION OF THE X-RAY CONTINUUM

Problems at low x-ray energies

Since continuum radiation is the principal constituent of the background for energies above 800 eV, considerable efforts have been made to represent its shape accurately. However, Russ[1] examined the effectiveness

* For Part 1 see Ref. 4.

CCC-0049–8246/85/0014–0008$04.00

© Wiley Heyden Ltd, 1985

of established methods of calculating the continuum and concluded that they are inadequate below 3 keV. This view was substantiated by Statham[8] who, despite much work on the nature of the continuum, found it extremely difficult to predict in the region below 2 keV. The situation becomes worse when carrying out soft x-ray analysis with 'windowless' detectors[3] because the continuum becomes larger and its curvature more pronounced. An additional complication is that calculation of the continuum requires a knowledge of the absorption characteristics of any detector window employed and of surface layers on the Si(Li) crystal itself. Furthermore, absorption may alter if significant contamination occurs on these surfaces from condensation of vapours present in the vacuum system,[9] or when the thin plastic detector window is replaced by another.

Reference standard method of Smith and co-workers[10–12]

A novel approach to continuum modelling, which eliminates the need to establish the absorption characteristics of the detector, has been proposed by Smith and co-workers.[10–12]

A continuum spectrum from a reference standard is first obtained and corrected channel by channel for all specimen-dependent effects; this is analogous to the atomic number and absorption corrections used in the conventional ZAF approach for characteristic radiations. The resulting spectrum represents the continuum, from a hypothetical specimen of atomic number $Z = 1$ producing no electron backscattering or x-ray absorption, as recorded by the ED detector (i.e. the true distribution modified by the spectrometer efficiency). Smith and co-workers termed this the 'normalized background,' but we prefer 'normalized continuum.' The continuum intensity for the sample of interest is then determined by carrying out the same procedure in reverse, on this occasion applying the relevant atomic number and absorption corrections for the sample, to the normalized continuum. Because the sample composition is not known initially, an estimate is made and then refined using an iterative procedure. An advantage of the method of Smith and co-workers, especially important with soft x-ray analysis, is that the detector efficiency is incorporated in the spectrum obtained from the reference specimen and therefore need not be explicitly known. Moreover, any change in detector efficiency may be easily taken into account by rerecording the reference spectrum.

In order to correct the continuum distribution for absorption effects, Smith and co-workers used a method commonly employed in ZAF programs, namely that of Philbert.[13] The absorption factor, $f(\chi)$ is given by

$$f(\chi) = \left[(1+\chi/\sigma)\left(1+\frac{h}{1+h}\,\chi/\sigma\right)\right]^{-1}$$

In this equation, $h = 1.2A/Z^2$, where A and Z represent the mean atomic weight and mean atomic number of the specimen, respectively; $\sigma = 4.5 \times 10^5/(E_0^{1.65} - E_\nu^{1.65})$, where E_0 is the incident electron energy and E_ν is the energy of the continuum radiation being corrected for absorption; and $\chi = (\mu/\rho)_{E_\nu}$ cosec θ, where θ is the x-ray take-off angle and $(\mu/\rho)_{E_\nu}$ is the mass absorption coefficient for x-rays of energy E_ν in the specimen.

The atomic number correction for the continuum was treated by Smith and co-workers in two parts. Firstly, losses in continuum production arising from electron backscattering were calculated using backscatter factors (R) values given by Rao-Sahib and Wittry.[14] Secondly, a correction factor, analogous to the stopping power factor (S) used in the conventional ZAF correction theory for characteristic radiation, was determined. The latter factor involves the efficiency with which electrons remaining in the specimen produce x-rays and is dependent on the energy of the electron at each point along its path and the corresponding cross-section for x-ray generation. Early theoretical work by Kramers[15] based on the Thompson–Whiddington law for electron retardation and a mainly classical approach to the calculation of the scattering cross section led to

$$I_\nu = KZ\frac{(E_0 - E_\nu)}{E_\nu}$$

where I_ν refers to the number of continuum x-rays with energy E_ν generated per second per electron, E_0 is the incident beam energy and K is a constant. Smith and co-workers found that this expression was not sufficiently accurate and investigated the use of a modified version, derived by Rao-Sahib and Wittry[14] using the Sommerfeld cross-section and Bethe retardation law:

$$I_\nu = KZ^n\left(\frac{E_0 - E_\nu}{E_\nu}\right)^X \qquad (1)$$

with $X = 1.11$ and n ranging from 1.2 to 1.37 depending on Z, E_0 and E_ν. Smith and co-workers reported initially[10,11] that X was close to unity and

$$n = 1.159 + (0.1239 - 0.02857 \ln E_0)(E_\nu - 2.044) \qquad (2)$$

but in later work[12] new expressions for X and n were given, both being functions of Z, E_0 and E_ν.

Development of the reference standard method for soft x-rays

The method of Smith and co-workers, to our knowledge, has not been used to predict the shape of the x-ray continuum below 1 keV. In order to extend its range of applicability to this region, further development was carried out on appropriate absorption and atomic number corrections. These corrections were then applied to spectra from various specimens, to determine the best method for obtaining normalized continuum spectra. Finally, this technique was combined with methods for dealing with artefacts[4] to predict complete spectral backgrounds which extend down to 0.1 keV.

Matrix absorption. Instead of using the Philibert absorption correction, it was decided to adopt the method of Love and Scott[16] since the latter should be more accurate when dealing with low-energy x-rays and large absorption effects. Here the absorption correction is given by

$$f(\chi)=\frac{1-\exp(-2\chi\overline{\rho z})}{2\chi\overline{\rho z}}$$

where $\overline{\rho z}$ is the mean depth of x-ray generation and is represented in terms of the electron backscatter coefficient, the maximum path length of an electron in the specimen and the overvoltage ratio (E_0/E_v). As with the Philibert model, the Love–Scott absorption correction was designed to deal with characteristic radiation rather than continuum. The distribution with depth in the specimen of continuum x-rays is, however, slightly different from characteristic x-rays, the mean depth of x-ray production being slightly larger for the former.[17] Fortunately, the two distributions are of similar shape and therefore until continuum distributions are known with greater certainty the mean depth appropriate for characteristic radiation has been used in the above equation for $f(\chi)$.

In order to apply the absorption correction the matrix mass absorption coefficient is required for each spectrum channel energy. For energies above 1.2 keV the empirical expression $\mu/\rho = C\lambda^n$ is often used, where λ is the x-ray wavelength, n is a constant between a particular set of absorption edges and C is a function of the absorber and the set of absorption edges bounding λ; tabulations of C and n have been produced by Heinrich.[18]

Although soft x-ray absorption coefficients for most characteristic line energies have been determined by Henke and Ebisu,[19] no expressions exist for calculating intermediate values. A non-linear regression algorithm[20] was therefore used to generate polynomial least-squares approximations to these data. Initial attempts using polynomials in energy (E) were found to give poor agreement with experimental results unless the order was at least as high as five. This is illustrated in plots of μ/ρ versus energy (Fig. 1(a) and (b)), where third- and fifth-order polynomial expressions are compared with the absorption coefficients in silicon. RMS percentage errors are 30 and 6, respectively. Even the fifth-order polynomial shows poor agreement and whilst polynomials of higher order produce less deviation they still behave erratically between data points. Clearly a different approach is required if the desired accuracy of *ca* 1% is to be achieved. The method finally adopted uses a third-order polynomial in E^P rather than E. Least-squares regression analysis indicated the optimum value for silicon was $P=-1.14$. Figure 1(d), the third-order polynomial fit, shows that the curve is well behaved and that there is good agreement (RMS percentage error 0.8) with the results of Henke and Ebisu. A full set of polynomial parameters for each element was obtained in a similar manner. These data were then combined with the C and n tabulation of Heinrich (suitable for x-rays >1.2 keV) to provide a means of rapidly calculating absorption coefficients for a range of x-ray energies from 0.1 to 25 keV in any element.

This data base for mass absorption coefficients was combined with the Love–Scott absorption model into a computer program to correct, sequentially, each spectrum channel for the effects of absorption by the matrix.

Atomic number effects. Unlike the backscatter corrections used in conventional ZAF procedures, which relate to characteristic radiation, the R values given by Rao-Sahib and Wittry[14] were determined specifically for continuum radiations. This suggests that they would be particularly useful in this work but, unfortunately, these R values cover a limited range of overvoltage (E_0/E_v) from 1 to 10. Thus when working with a 15 keV probe, R values will not be available below 1.5 keV. Extrapolation to lower energies would be possible but could introduce errors when considering energies as low as 0.1 keV. The alternative was to use a backscatter factor for characteristic radiation which was applicable to the low energy region. It appears

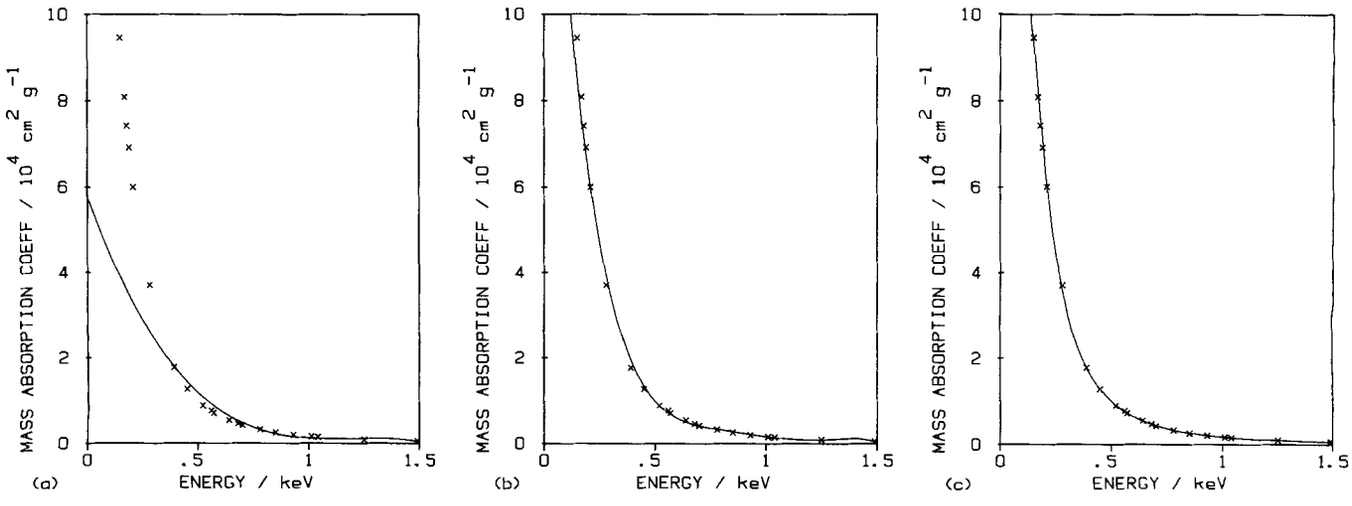

Figure 1. Mass absorption coefficient for silicon absorber. ×, Experimental data from Henke and Ebisu.[19] Curves, polynomial least-squares approximations. (a) Third order in E; (b) fifth order in E; and (c) third order in $E^{-1.14}$.

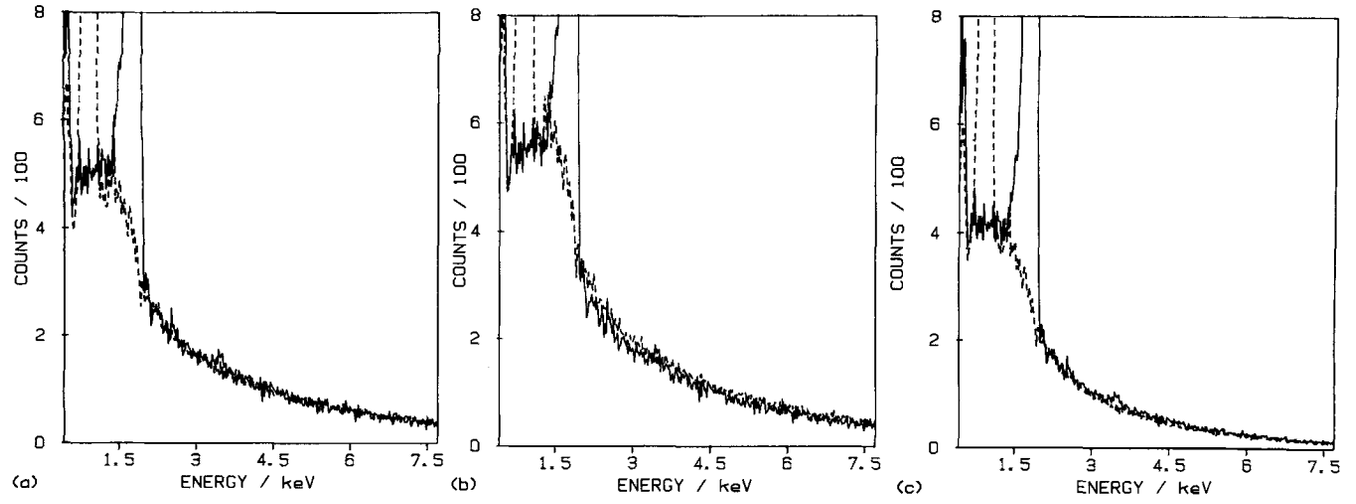

Figure 2. Comparison of spectra from silicon (solid curve) and copper (broken curve) after dividing through by absorption factor and (a) Z, (b) backscatter factor and Z and (c) backscatter factor and Smith and co-workers, Z^n factor. Formvar window, 15 kV.

that R values given by the approach of Love and co-workers[16,21] agree well with those of Duncumb and Reed[22] and are in fact very similar to those for continuum given by Rao-Sahib and Wittry.[14] We therefore decided to use the method developed by Love and co-workers in which R is calculated from the backscatter coefficient (η) in the expression

$$R = 1 - \eta[I(U_0) + \eta G(U_0)]^{1.67}$$

where I and G are functions of overvoltage U_0 ($U_0 = E_0/E_\nu$) and η is determined from an expression involving Z and E_0.

Two methods of correcting for atomic number were investigated. The first was to use Eqn (1) taking X as unity, as proposed by Smith and co-workers, giving a dependence of I_ν upon Z^n with n calculated for each channel energy from Eqn (2). The second involved setting n equal to unity, which effectively assumes a dependence of I_ν on Z as given by Kramers' law.

Obtaining normalized continuum spectra. The correction factors discussed in the two previous sections were used, individually and collectively, on continuum spectra from a range of specimens. The results indicated that because of the strong influence of absorption edges, the absorption correction was most significant in correcting the continuum shape. Spectra corrected only for absorption showed large differences in size, but these were found to be very nearly proportional to atomic number Z. Thus channel by channel division of spectra by the absorption factors and Z (equivalent to the use of Kramers' law) appeared to be successful in eliminating specimen dependent effects. This is illustrated in Fig. 2(a), for silicon and copper specimens, showing good agreement between the continuum levels in the corrected spectra. Figure 2(b) shows the result of a further division by backscatter factors, giving a slightly poorer agreement.

If the absorption and backscatter corrections are retained, but the Z factor replaced by the Z^n term proposed by Smith and co-workers, then good agreement is again achieved, as shown in Fig. 2(c).

The corrections for backscattering would be expected to become more significant as the difference in specimen atomic number is increased. This was found to be the case. Figure 3(a) shows the result of dividing silicon and tin spectra by absorption factors and Z; it is apparent that the continuum from tin is reduced at

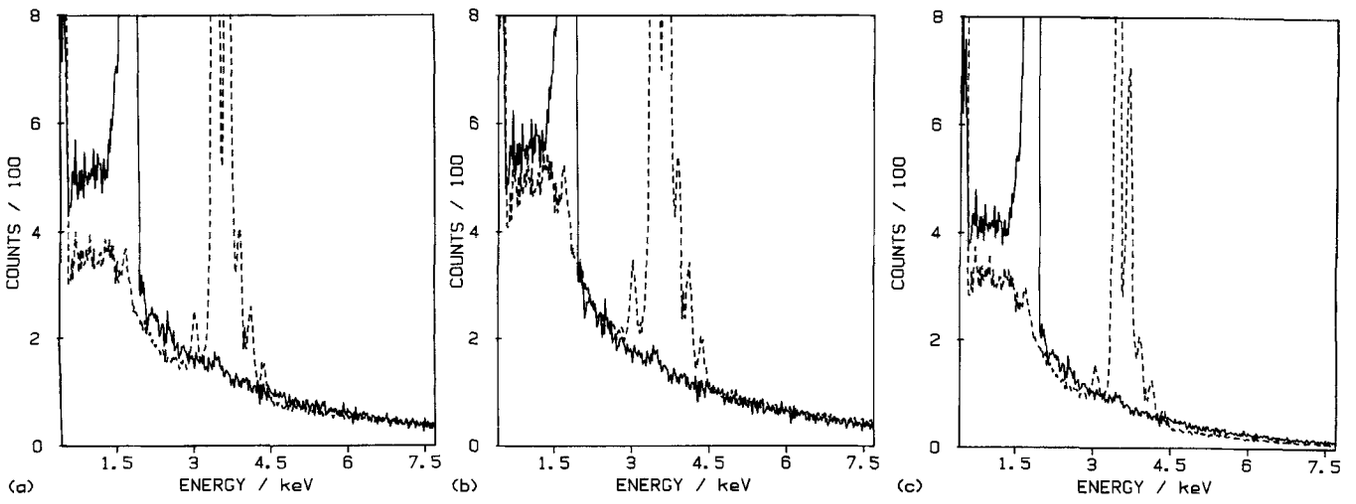

Figure 3. As Fig. 2 but for silicon (solid curve) and tin (broken curve).

low energies owing to greater backscattering loses. Additional use of a backscatter correction for each spectrum improves the agreement, as shown in Fig. 3(b). If, however, the Z term is replaced by the Z^n of Smith and co-workers the agreement becomes worse again, as in Fig. 3(c).

Similar results were obtained with other specimens and probe voltages. It was therefore concluded that channel by channel division by the absorption factor and Z could be used to produce a 'normalized continuum' spectrum from a given standard. This normalized spectrum would then be correct for other specimens over a useful range of atomic numbers, such as $Z/2$ to $2Z$. Further, a wider range of validity can be achieved, if necessary, by use of the backscatter correction, although when using this technique for continuum prediction it is generally advisable to select a reference standard which is reasonably close in atomic number to the specimen being analysed.

Use of the reference standard method. First a standard is required to give a reference spectrum which does not contain peaks in the energy range of interest (0–1 keV in light element analysis). Silicon is a good choice, although if the specimen has a high mean atomic number it may be preferable to select a heavier element in order to minimize errors in calculating the background.

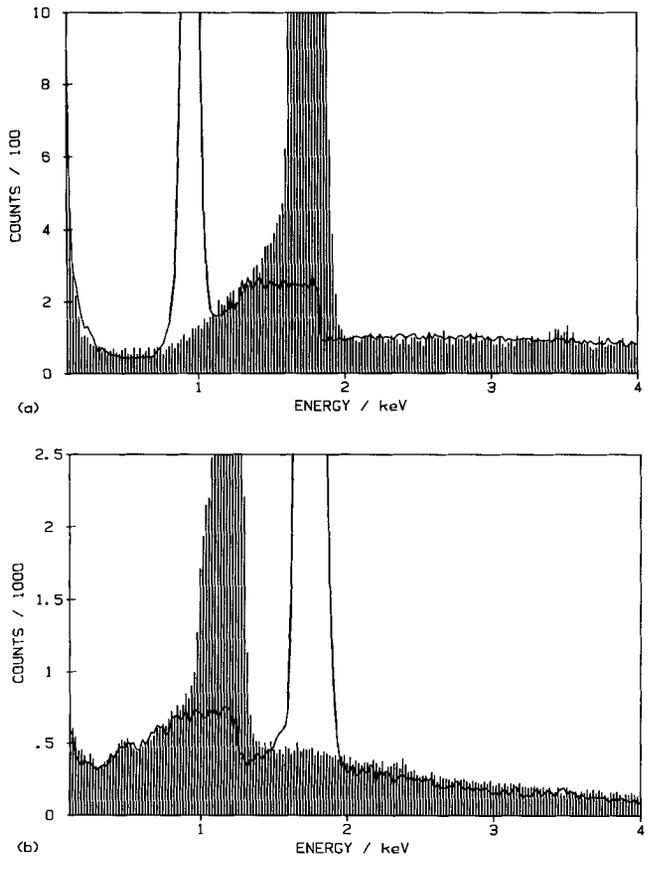

Figure 4. Calculated backgrounds (continuous lines) based on the continuum reference method. (a) Specimen, silicon; reference standard, copper; beryllium window, 15 kV. (b) Specimen, germanium; reference standard, silicon; Formvar window, 7 kV.

The reference spectrum is obtained at the same accelerating voltage and sample inclination used when recording the spectrum from the specimen; live time is determined and both noise and spur artefacts subtracted (see Ref. 4). Next, the continuum is modified as described earlier, to take account of the different absorption and atomic number of specimen and standard. Finally, the background of the specimen is completed by adding to the continuum the appropriate contributions from noise and spur.

Backgrounds calculated using this procedure are illustrated in Fig. 4(a) and (b) for specimens of silicon and germanium, respectively. The calculated backgrounds agree well with experimental data over this energy range even when the reference standard and specimen differ widely in atomic number. Figure 5 shows a practical example of the technique applied to a spectrum containing low concentrations of light elements, in this instance from carbon and oxygen in a contamination layer on the surface of aluminium. It should be noted that the background beneath the carbon peak (Fig. 5(a)) is very different from that given by linear interpolation and that after background subtraction (Fig. 5(b)) both carbon and oxygen peaks are clearly resolved.

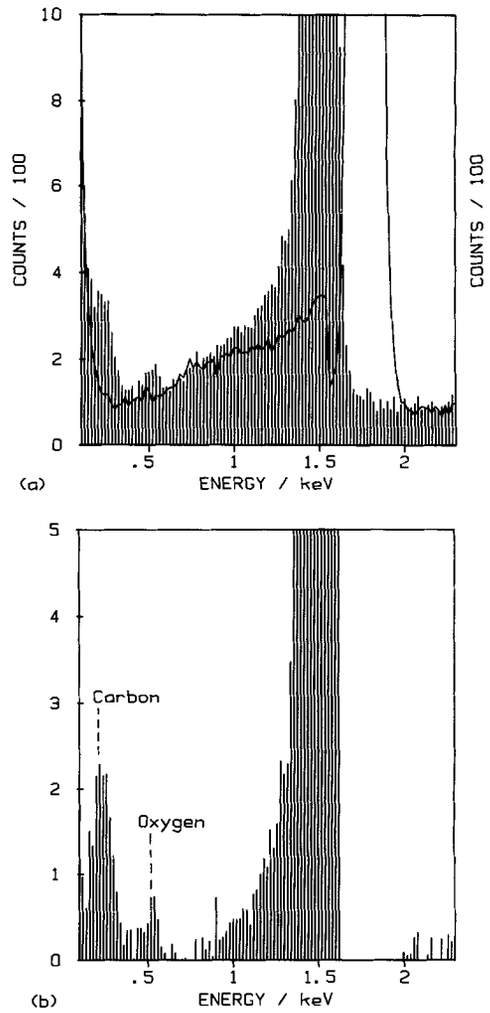

Figure 5. Spectrum from contaminated aluminium specimen; Formvar window, 15 kV. (a) Continuous line shows calculated background. (b) Spectrum with background removed.

PEAK OVERLAP

The problem of measuring overlapping peaks is basically the same for low- as for high-energy x-ray lines, the only difference being that low-energy peaks tend to be asymmetrical because incomplete charge collection results in a low-energy tail.[2]

The two commonest methods for dealing with peak overlap use overlap factors or peak fitting, both of which will now be discussed and compared.

Overlap factors

Overlap factors represent the fraction of integrated peak intensity of one element which appears in the region over which the neighbouring peak is integrated. For example, in Fig. 6, the factor describing the overlap of peak A into the integration region of B (denoted by ab) is given by Y/X. If these are known, true peak intensities may be established from uncorrected intensities by means of an iterative procedure. When, however, three or more peaks are involved the situation becomes complicated and is more easily solved by using a set of simultaneous equations:

$$A + Bba + Cca = S_1$$
$$Aab + B + Ccb = S_2$$
$$Aac + Bbc + C = S_3$$

where S_1, S_2 and S_3 are the measured integrals at peak positions and A, B and C are unknown peak integrals. These equations can be expressed in matrix notation as follows:

$$\begin{bmatrix} 1 & ba & ca \\ ab & 1 & cb \\ ac & bc & 1 \end{bmatrix} * \begin{bmatrix} A \\ B \\ C \end{bmatrix} = \begin{bmatrix} S_1 \\ S_2 \\ S_3 \end{bmatrix}$$

or rewritten in the more general form

$$P_{ij}I_i = S_j \qquad (3)$$

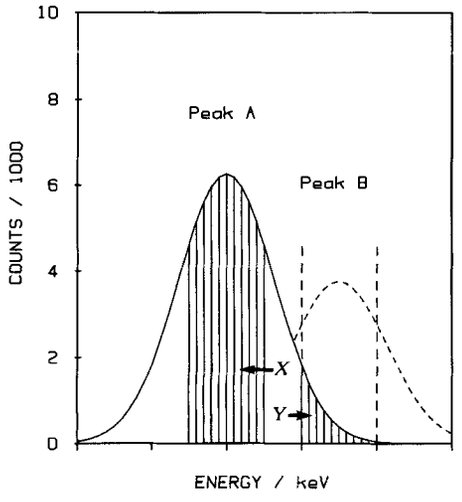

Figure 6. Schematic diagram showing the integration region (X) of peak A and the overlap (Y) of A into the integration region of peak B.

where $1 \leqslant i \leqslant 3$ and $1 \leqslant j \leqslant 3$. Now a solution may be obtained by, for example, inversion of the P matrix in Eqn (3).

Peak fitting

The treatment outlined above may be extended by increasing the size of the matrix so that $1 \leqslant i \leqslant n$ and $1 \leqslant j \leqslant m$, then a complete band of the spectrum (after background removal) may be represented as the sum of a series of characteristic peaks. Equation (3) is still applicable but now S_j is a portion of spectrum containing m channels and the n columns of P_{ij} are the various components of the spectrum, the size of each component being I_i. Thus the count in the jth channel of the spectrum S_j is given by

$$S_j = \sum_{i=1}^{n} P_{ij}I_i$$

It follows that the method of overlap factors is merely a simplified version of this more general treatment. When overlap factors are employed, P_{ij} represents counts integrated over a number of channels of the spectrum, the integration bands being centred at the position of each peak. In this case P_{ij} is a square matrix and Eqn (3) has a unique solution. Since statistical errors affect results directly, those associated with the spectral background are minimized by keeping the integration bands narrow ($\sim\frac{1}{2}$FWHM; FWHM = full width at half maximum intensity). In the general treatment the actual components of spectrum P_{ij} are not simply overlap values but representations of peak shapes. Approximations to these shapes can be obtained from experimental or model peak shapes, M_{ij}. Equation (3) becomes

$$M_{ij}I_i \simeq S_j \qquad (4)$$

which consists of m equations in n unknowns. This has many possible solutions, but the one generally chosen is that which minimizes the sum of the squared errors for each j, i.e. the least-squares fit of M_{ij} to S_j. Channel counts from tails of peaks may be included for fitting purposes since, despite poor statistics, they provide additional information. Thus, the general approach is capable of treating peaks over their full width, thereby offering potentially greater accuracy than the method of overlap factors. An additional advantage is that the results of the fit $M_{ij} \times I_i$ can be calculated and compared directly with the original spectrum S_j.

Fitting requires a knowledge of peak shapes, and this is most easily attained by storing relevant spectra (with background removed) from standard specimens. It would be possible to use mathematically generated Gaussian shapes, but these have to be compared with experimental peaks at some stage to ensure that they provide a sufficiently accurate representation. Also, in the low-energy region (0.1–1 keV) peaks tend to be asymmetrical and difficult to model; consequently, it was decided to use experimentally recorded spectra for deconvolution purposes.

The least-squares solution. One way of solving Eqn (4)

is to multiply both sides by an $m \times n$ matrix, Q_{ji}, i.e.

$$Q_{ji}M_{ij}I_i = Q_{ji}S_j \quad (5)$$

QM is an $n \times n$ matrix and so the above expression represents n equations in n unknowns and generally has a unique solution. The choice of Q_{ji} is, however, arbitrary and each Q_{ji} matrix will result in a different solution. The least-squares solution (I_i) to Eqn (4) is the one which minimizes

$$\sum_j \left(S_j - \sum_i M_{ij}I_i\right)^2 \quad (6)$$

This result will be obtained from Eqn (5) if $Q_{ji} = M_{ij}{}^T$, where $M_{ij}{}^T$ is the transpose of matrix M_{ij} (see Ref. 20). Since M^TM is an $n \times n$ matrix it generally has an inverse, in which case the solution can be expressed by

$$I = [M^TM]^{-1}M^TS \quad (7)$$

This inverse matrix may be calculated in several ways,[23] but it is generally accepted that inversion is prone to computational errors in certain situations.[20]

A more reliable method for solving Eqn (4) is to use singular value decomposition (SVD), which generates a pseudo inverse M^+ such that

$$I = M^+S \quad (8)$$

is the least-squares solution. The SVD method can be implemented in various ways[24] to suit the requirements of speed and available computer memory.

In addition to computational accuracy, there are two other requirements to be taken into account when choosing an algorithm for solving Eqn (4). Firstly, statistical accuracies of channel values are not constant but are given by $\sigma_{sj} \simeq \sqrt{S_j}$, where S_j is the count in the jth channel. Hence, it is more appropriate to use a modified form of expression (6) and minimize

$$\sum_j \left[\frac{S_j - \sum_i M_{ij}I_i}{\sigma_{sj}}\right]^2$$

Secondly, it is important to calculate the statistical accuracy of the resulting fit. This depends on counting statistics in the spectrum from the specimen and the mathematical operations used to calculate the results. For example, in Eqns (7) and (8) the solution can be written as

$$I_i = X_{ji}S_j$$

where X_{ji} is derived in some manner from the standard or model peak shapes M_{ij}. If statistical errors in M_{ij} are small compared with those in the spectrum S_j, then errors σ_{Ii} in I_i can be calculated as

$$\sigma_{Ii} = \sqrt{\sum (X_{ji}\sigma_{sj})^2}$$

Furthermore, if σ_{sj} is approximated by $\sqrt{S_j}$, then

$$\sigma_{Ii} = \sqrt{\sum (X_{ji}{}^2 S_j)}$$

Assessment of peak deconvolution by least-squares fitting. Matrix inversion and SVD methods of solving Eqn (4) were examined by use of simple Gaussian shapes added together in known proportions to simulate a variety of overlap situtations. Computer programs were written to calculate least-squares fits of the original Gaussian shapes to the overlap. Options to apply the necessary weighting and to calculate statistical errors in the final results were incorporated in both matrix inversion and SVD programs. Computational accuracy was also checked by comparing the results of the fit with the known sizes of the original Gaussian shapes.

In all cases, the simple matrix inversion and SVD method gave similar predictions of statistical error, but the SVD approach incurred consistently lower computational errors. Nevertheless, statistical errors were always at least 100 times greater than the computational ones, so the matrix inversion technique is still perfectly adequate in this type of application. The choice of which technique to use therefore depends largely on which is most convenient to implement. Matrix inversion was selected here because matrix handling routines were already available on the Data General computer used in this work.

Statistical errors arising from the deconvolution of two peaks with centroids separated by varying amounts have been evaluated. Matrix inversion was used to deconvolute a Gaussian peak with 10 000 counts and an FWHM of 120 eV from (a) a neighbouring peak of the same magnitude, (b) a peak of 250 000 counts and (c) a peak of 250 000 counts and a background of 15 000 counts per 20 eV channel. The relative sizes of these peaks and the background are illustrated in Fig. 7. The results of the deconvolution are shown in Fig. 8 plotted as percentage statistical error versus peak separation. It is evident that a 10 000 count peak which is overlapped by a similar size peak can be resolved with only 5% error when the separation is as little as 20 eV, provided that the background is low. In extremely difficult situations, when a large neighbouring peak and high background level are present, the statistical errors are greater, being 10% for a peak separation of 80 eV.

These results represent the limit of accuracy that can be achieved under ideal conditions; in practice, changes in resolution or peak position will cause addi-

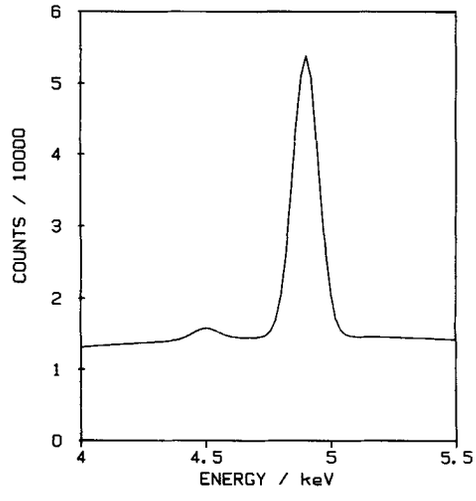

Figure 7. Relative sizes of peaks with 10 000 and 250 000 integrated counts and a background of 15 000 counts; 20 eV per channel.

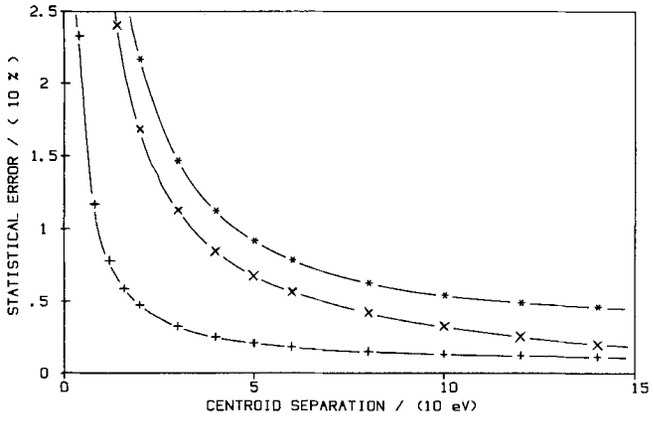

Figure 8. Statistical error vs peak separation for deconvolution of a peak (10 000 integrated counts, FWHM 120 eV) from a peak of the same size (+), a peak of 250 000 integrated counts (×) and a 250 000 count peak with a 15 000 count background level (*). 20 eV per channel.

tional errors. Non-linear fitting techniques which compensate for such changes have been described;[25] they search for progressive improvements in the fit by adjusting the peak parameters until the optimum positions, widths and sizes are found. Whilst this is most directly applicable when fitting mathematical peak models, a certain amount of 'peak shape manipulation' is possible even when experimental spectra from standards are used. In simple overlap situations the ability to correct for a change in peak position would be useful, but Statham[26] has shown that in severe overlaps the non-linear approach can sometimes produce large errors. Further investigation[27] has shown that although the occurrence of such errors is unlikely, it remains difficult to ensure the reliability of non-linear fitting. Furthermore, changes in resolution and peak position are not inherent in the analysis technique but depend on the stability of the electronic equipment.

CONCLUSIONS

Prediction of the continuum in ED spectra has been examined with particular attention to energies below 1.5 keV and a satisfactory approach has been found. Then, by summing the contributions from continuum and spectrum artefacts the background down to 0.1 keV may be determined.

Deconvolution of peak overlap has been discussed, including the application of different mathematical techniques, incorporation of weighting and calculation of statistical errors. Studies have shown that the magnitudes of errors in most practical situations will be 5–10%.

Non-linear fitting has been considered, but owing to its inherent lack of reliability it has not been used in this work. In practical situations the emphasis will be placed on careful calibration of the system and analysis of specimens and standards within short time periods to minimize any changes in resolution and peak position.

In a subsequent paper the methods of spectrum processing developed in this paper will be used to assess the sensitivity of light element ED analysis and the feasibility of quantitative measurements.

Acknowledgements

Thanks are due to the SERC and the Procurement Executive, MOD, for their support of this work.

REFERENCES

1. J. C. Russ, *X-Ray Spectrom.* **6**, 37 (1977).
2. P. J. Statham, *J. Microsc.* **123**, 1 (1981).
3. J. C. Russ, in *Scanning Electron Microscopy*, edited by O. M. Johari, Vol. 1, p. 298. SEM Inc., Chicago, IL (1977).
4. D. J. Bloomfield, G. Love and V. D. Scott, *X-Ray Spectrom.* **13**, 69 (1984).
5. P. J. Statham, Anal. Chem. *49*(14), 2149 *13*(2), 69 (1984).
6. J. J. McCarthy and F. H. Schamber, in *Energy Dispersive X-Ray Spectrometry*, edited by K. F. J. Heinrich, D. E. Newbury, R. L. Myklebust and C. E. Fiori, NBS Special Publication No. 604, pp. 273–296. National Bureau of Standards, Washington, DC (1981).
7. N. G. Ware and S. J. B. Reed, *J. Phys. E* **6**, 286 (1973).
8. P. J. Statham, *X-Ray Spectrom.* **5**, 154 (1976).
9. G. Love, V. D. Scott, N. M. T. Dennis and L. Laurenson, *Scanning* **4**, 32 (1981).
10. D. G. W. Smith, C. M. Gold and D. A. Tomlinson, *X-Ray Spectrom.* **4**, 149 (1975).
11. D. G. W. Smith and C. M. Gold, *Adv. X-Ray Anal.* **19**, 191 (1976).
12. D. G. W. Smith and C. M. Gold, in *Microbeam Analysis*, edited by D. E. Newbury, p. 273. San Francisco Press, San Francisco (1979).
13. J. Philibert, in *X-Ray Optics and X-Ray Microanalysis*, edited by H. H. Patee, V. E. Cosslett and A. Engstrom, pp. 379–392. Academic Press, New York (1963).
14. T. S. Rao-Sahib and D. B. Wittry, *J. Appl. Phys.* **45**, 5060 (1974).
15. H. A. Kramers, *Philos. Mag.* **46**, 836 (1932).
16. G. Love and V. D. Scott, *J. Phys. D* **11**, 1369 (1978).
17. S. J. B. Reed, *X-Ray Spectrom.* **4**, 14 (1975).
18. K. F. J. Heinrich, in *The Electron Microprobe*, edited by T. D. McKinley, K. F. J. Heinrich and D. B. Wittry, pp. 296–377. Wiley, New York (1966).
19. B. L. Henke and E. S. Ebisu, *Adv. X-Ray Anal.* **17**, 150 (1973).
20. A. Ralston and P. Rabinowitz, *A First Course in Numerical Analysis*, 2nd ed. McGraw-Hill, New York (1978).
21. G. Love, M. G. C. Cox and V. D. Scott, *J. Phys. D* **11**, 7 (1978).
22. P. Duncumb and S. J. B. Reed, in *Quantitative Electron Probe Microanalysis*, edited by K. F. J. Heinrich, NBS Special Publication No. 298, pp. 133–154. National Bureau of Standards, Washington, DC (1968).
23. J. R. Westlake, *A Handbook of Numerical Matrix Inversion and Solutions of Linear Equations.* Wiley, New York (1968).
24. J. C. Nash, *Compact Numerical Methods for Computers: Linear Algebra and Function Minimisation.* Adam Hilger, Bristol (1979).
25. C. E. Fiori, R. L. Myklebust and K. Gorlen, in *Energy Dispersive X-Ray Spectrometry*, edited by K. F. J. Heinrich, D. E. Newbury, R. L. Myklebust and C. E. Fiori, NBS Special Publication No. 604, pp. 233–272. National Bureau of Standards, Washington, DC (1981).
26. P. J. Statham, *X-Ray Spectrom.* **7**, 132 (1978).
27. F. H. Schamber, in *Energy Dispersive X-Ray Spectrometry*, edited by K. F. J. Heinrich, D. E. Newbury, R. L. Myklebust and C. E. Fiori, NBS Special Publication No. 604, pp. 193–231. National Bureau of Standards, Washington, DC (1981).

Received 5 August 1983; accepted 7 March 1984